Supplementary Information (SI) for Dalton Transactions.
This journal is © The Royal Society of Chemistry 2025

Efficient degradation of tetracycline hydrochloride by activation of peroxomonosulfate on magnetic steel slag/MoS_2 composite via ball milling

Caihong Fang, Longhui Nie*, Ruihao Li, Yiting Zheng

(School of Materials and Chemical Engineering, Hubei University of Technology, Wuhan 430068, China)

** Author to whom any correspondence should be addressed. E-mail: nielonghui@mail.hbut.edu.cn (L. Nie)*

1. Experimental section

1.1 Experimental steps for active species quenching

To further investigate the active species of the MSS@MoS_2-50/PMS system, active species quenching experiments were used to probe the presence of reactive species in the system. In this work, methanol (MeOH), isopropanol (IPA), p-benzoquinone (p-BQ), and furfuryl alcohol (FFA) were used as trapping agents for ・SO_4^{2-}, -OH, ・O_2^-, and $^1O_2$, respectively. The catalyst sample (0.02 g) was dispersed in TCH aqueous solution (50 ml, 70 mg/L) in four 150 mL conical flasks. After 30-minute adsorption, the adsorption equilibrium was established. The quenching reagents (3 mL MeOH, 20 mmol IPA, 0.8 mmol p-BQ and 2 mmol FFA) and PMS (1 mmol/L) were added immediately to start the Fenton-like reaction. The next steps in the experiment are the same as those described in main text 2.3.

2. Results

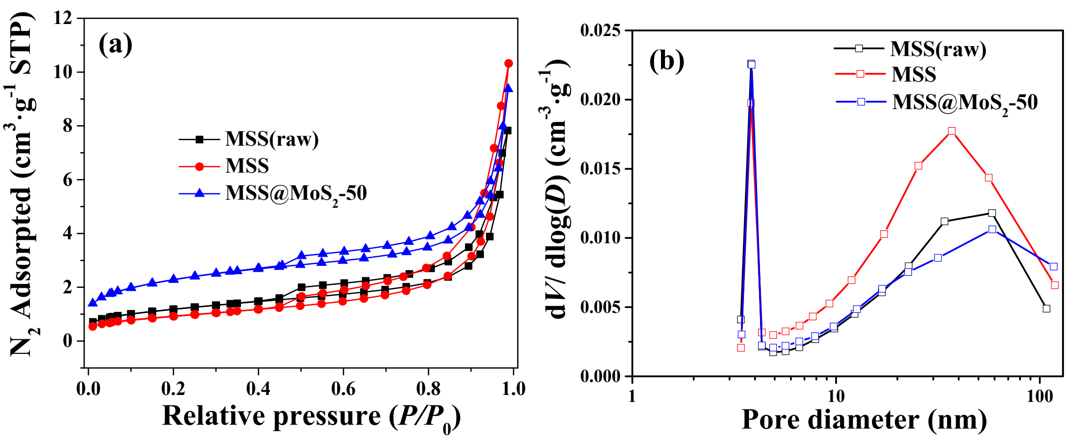

Fig. S1. N_2 adsorption/desorption isotherms (a) and the corresponding pore size distribution (b) for the raw MSS, MSS, and MSS@MoS_2-50 samples.

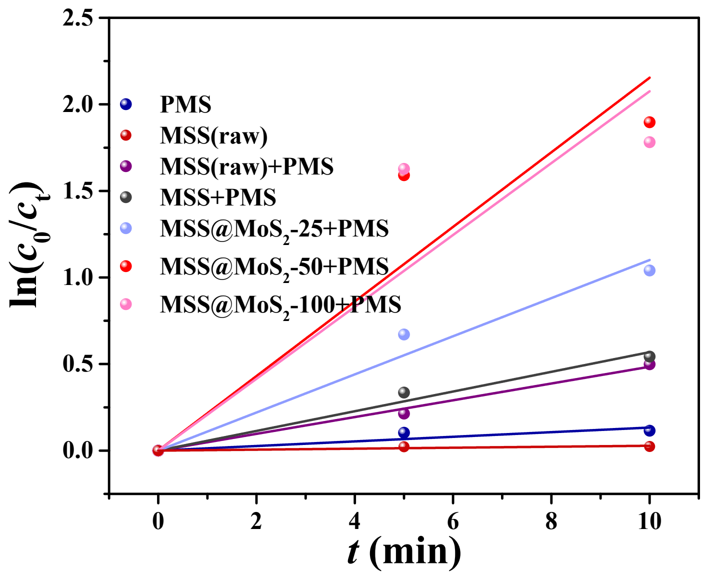

Fig. S2 The first-order-kinetics fitting of TCH degradation in different catalysts/PMS systems. ([catalyst dosage] =0.4 g/L, [PMS]=1 mM, [TCH]=70 mg/L, initial pH=4, temperature = 30 ^{o}C).

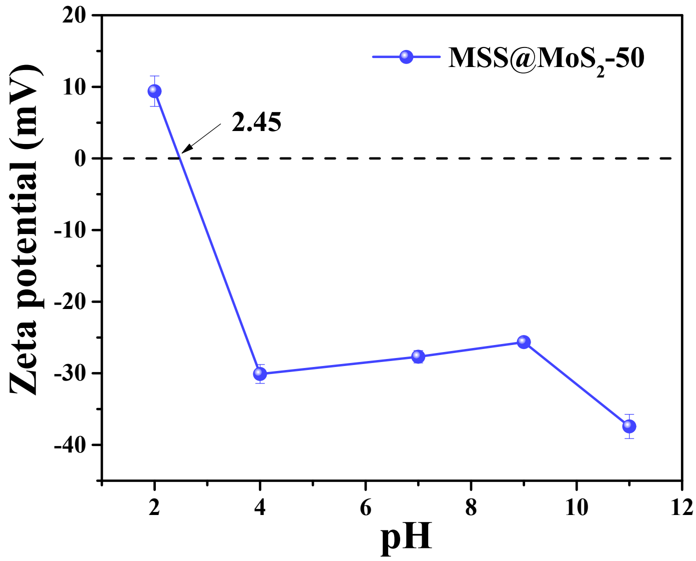

Fig. S3 Zeta potential dependence on pH for MSS@MoS_2-50.

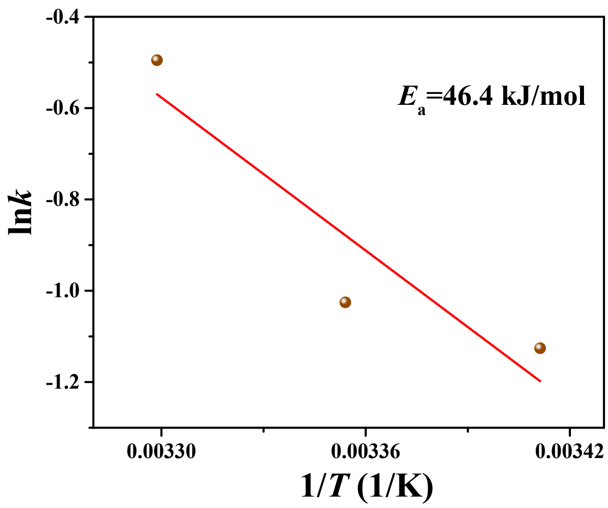

Fig. S4 Arrhenius plot for activation energy in the degradation of TCH by MSS@MoS_2-50 at different temperatures.

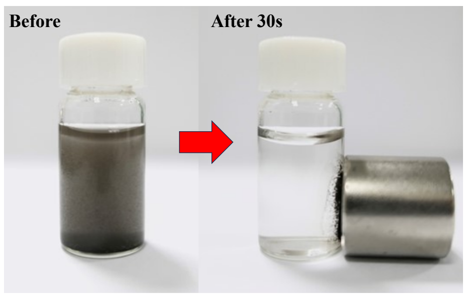

Fig. S5. Photo images of the MSS@MoS_2-50 suspension before and after magnetic separation

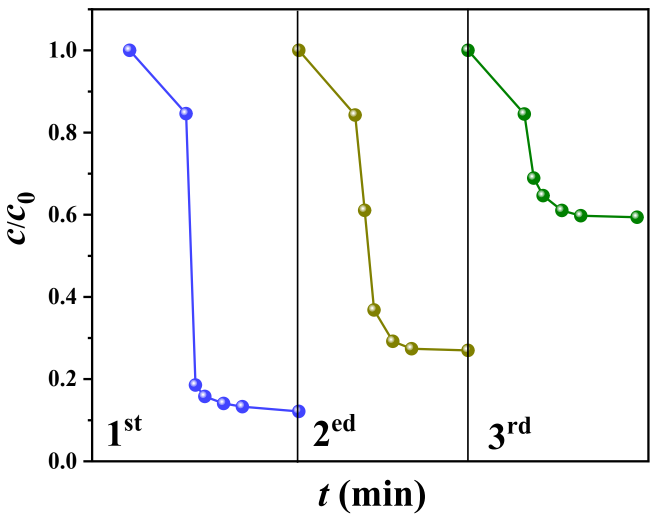

Fig. S6 The MSS (raw)@MoS_2-50/PMS system degradation of TCH after three cycles. ([catalyst dosage] = 0.4 g/L, [PMS]=1 mM, [TCH]=70 mg/L, initial pH=4, initial temperature = 30 °C).

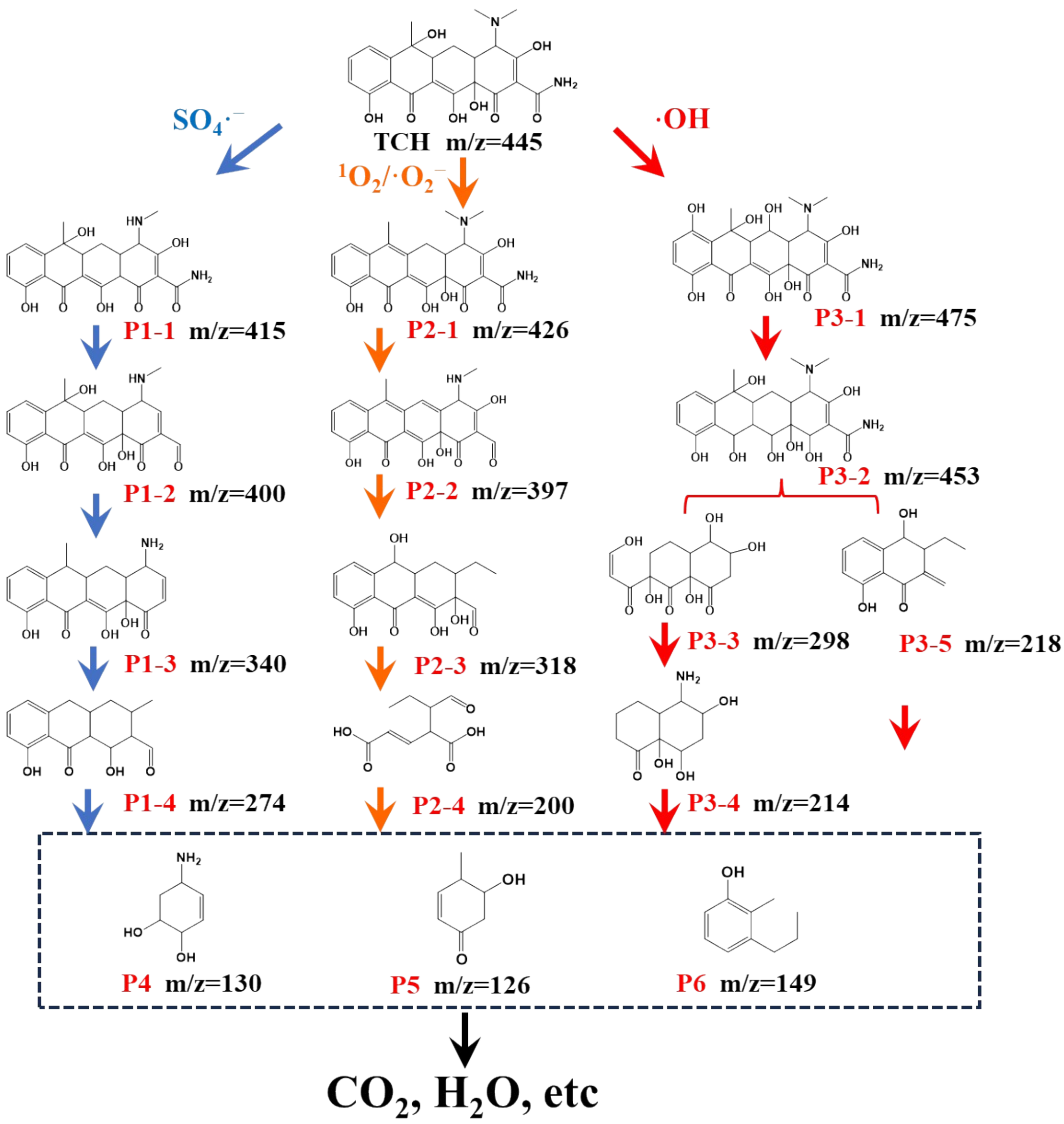

Fig. S7 Intermediates and three pathways for TCH degradation in MSS@MoS_2-50/PMS system.

Table S1 Mass percentages of main elements in raw MSS supposing they exist as metal oxides

SiO_2/wt%	Fe_2O_3/ wt %	CaO/ wt %	MgO/ wt %	Na_2O/ wt %	Al_2O_3/ wt %
12.64	25.44	38.02	3.91	2.89	4.06

Table S2 Specific surface area, pore volume, and pore size parameters of steel slag samples.

catalyst	S_{BET} ($m^2 \cdot g^{-1}$)	V_{pore} ($cm^3 \cdot g^{-1}$)	d_{pore} (nm)
MSS(raw)	4.3	0.01	3.8
MSS	3.3	0.02	3.8
MSS@MoS_2-50	8.1	0.01	3.9

Table S3 A comparison of catalytic activity between MSS@MoS_2-50 and those in the literature. (k_1 is the first-order rate constant; k_2 is the second-order rate constant)

Catalysts	Reaction conditions	Catalytic performance	Rate constant k_1 (min^{-1})/k_2 ($L \cdot mg^{-1} \cdot min^{-1}$)	References
MSS@Co-CN	pH: 4.0; Catalyst dosage: 0.6 g/L; [PMS]: 1 mM; C_0: 70 mg/L; t: 30 °C	90% removal in 30 min	/	[1]
Co-Fe@PPBC	pH: 3.0; Catalyst dosage: 0.1 g/L; [PMS]: 3.35 mM; C_0: 50 mg/L; t: 25 °C	78.0% removal in 30 min	k_1=0.3295	[2]
Fe-C_3N_4	pH:7; Catalyst dosage: 0.4 g/L; Light; C_0: 20 mg/L; t: 20 °C	94.0% removal in 180 min	k_1=0.0123	[3]
Co_9S_8	pH: 5.2; Catalyst: 0.1 g/L; [PMS]: 1.0 mM; C_0: 10 mg/L; t: 25 °C	88.2% removal in 30 min	k_1=0.121	[4]
0.6LDO/M-I	pH: 4.98; Catalyst: 0.4 g/L; [PMS]: / mM; C_0: 500 mg/L; t: 25 °C	92.92% removal in 25 min	k_2=1.4133	[5]
CuO-550	Catalyst: 0.2 g/L; [PMS]: 1 mM; C_0: 40 μM; t: 28 °C	100% removal in 40 min	k_1=0.1467	[6]
Fe/NC-30	pH: 6.6; Catalyst: 0.1 g/L; [PMS]: 0.2 mM; C_0: 10 mg/L; t: 25 °C	95.0% removal in 30 min	k_1=0.222	[7]
MM3	pH: 7.0; Catalyst: 0.2 g/L; [PMS]: 1.0 mM; C_0: 10 mg/L; t: 25 °C	92.9% removal in 30 min	k_1=0.150	[8]

C-Co-TN	pH: 4.6; Catalyst dosage: 0.1 g/L; [PMS]: 0.75 mM; C_0: 20 mg/L; *t*: 25 °C	93.3% removal in 30 min	k_1=0.042	[9]
MSS@MoS$_2$-0.01	pH: 4.0; Catalyst: 0.4 g/L; [PMS]: 1.0 mM; C_0: 70 mg/L; *t*: 30 °C	92.0% removal in 60 min, 82% in first 5 min	k_1=0.208, k_2=10.59	This work

Table S4 The first-order-kinetics reaction rate constant (k_1) for different catalysts/PMS system

sample	k_1 (min^{-1})	R^2
PMS	0.013	0.931
MSS (raw)	0.003	0.922
MSS (raw)+PMS	0.048	0.997
MSS+PMS	0.057	0.992
MSS@MoS$_2$-25+PMS	0.110	0.988
MSS@MoS$_2$-50+PMS	0.208	0.925
MSS@MoS$_2$-100+PMS	0.188	0.929

Table S5 The pseudo-second-order-kinetics reaction rate constant (k_2) for different catalysts/PMS system

sample	k_2 (L·g^{-1}·min^{-1})	R^2
PMS	0.20	0.999
MSS (raw)	0.05	0.999
MSS (raw)+PMS	1.32	0.997
MSS+PMS	1.23	0.999
MSS@MoS$_2$-25+PMS	3.17	0.999
MSS@MoS$_2$-50+PMS	10.59	0.997
MSS@MoS$_2$-100+PMS	9.68	0.966

Table S6 Atomic percentage of each element in MSS@MoS_2-50 catalyst before and after the reaction from XPS.

Sample	Elements/ Atomic%				
	C 1s	Fe 2p	Mo 3d	O 1s	S 2p
Before	41.68	2.03	0.40	54.81	1.07
After	40.24	2.23	0.24	56.41	0.88

Table S7 TCH degradation intermediates in the MSS@MoS_2-50/PMS system.

Products	R.T.	*m*/*z*	Proposed structure
TCH		445	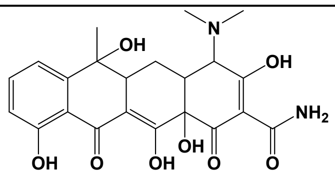
P1-1	11.41	415	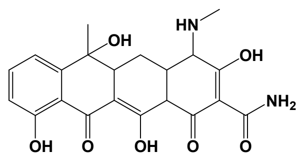
P1-2	7.02	400	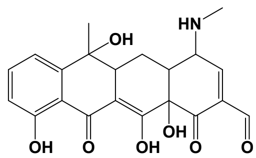
P1-3	4.54	340	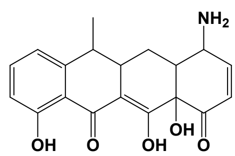
P1-4	9.60	274	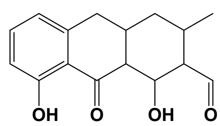
P2-1	7.02	426	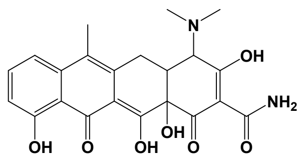
P2-2	6.49	397	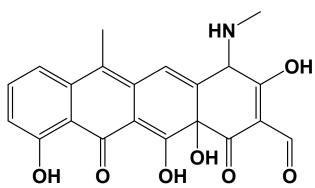

P2-3	9.60	318	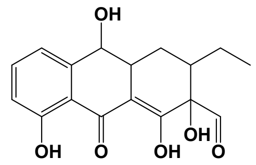
P2-4	8.46	200	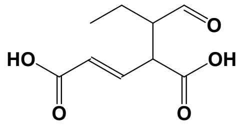
P3-1	5.44	475	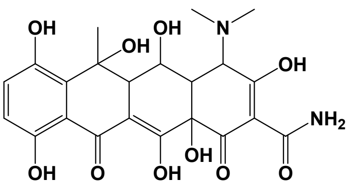
P3-2	5.44	453	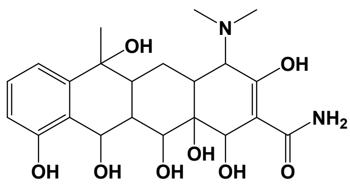
P3-3	11.41	298	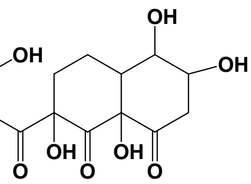
P3-4	0.67	214	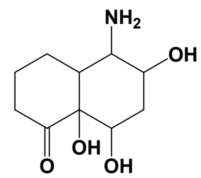
P3-5	6.74	218	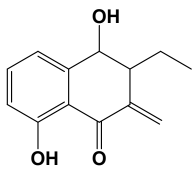
P4	4.96	130	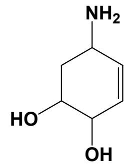
P5	0.67	126	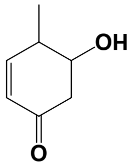
P6	5.05	149	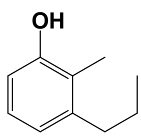

[1]. C. Fang, L. Nie, H. Chen, and Y. Yang, Magnetic recyclable Co-MOF derivate-modified steel slag for tetracycline removal by integrated adsorption and Fenton-like catalysis. Journal of Water Process Engineering. 63 (2024). https://doi.org/10.1016/j.jwpe.2024.105434

[2]. S. Han and P. Xiao, Catalytic degradation of tetracycline using peroxymonosulfate activated by cobalt and iron co-loaded pomelo peel biochar nanocomposite: Characterization, performance and reaction mechanism. Sep. Purif. Technol. 287 (2022) 120533. https://doi.org/10.1016/j.seppur.2022.120533

[3]. Y. Feng, Y. Liang, C. Ding, Y. Jiang, H. Jin, S. Rong, J. Wu, S. He, C. Xia, and L. Xue, Sustainable design of photo-Fenton-like oxidation process in actual livestock wastewater through the highly dispersed $FeCl_3$ anchoring on a g-C_3N_4 substrate. Water Research. 259 (2024). https://doi.org/10.1016/j.watres.2024.121889

[4]. G. Zhang, J. Gao, J. Wang, H. Lin, J. Xu, and L. Wang, ZIF-67/melamine derived hollow N-doped carbon/Co_9S_8 polyhedron to activate peroxymonosulfate for degradation of tetracycline. J. Environ. Chem. Eng. 11 (2023) 109355. https://doi.org/10.1016/j.jece.2023.109355

[5]. Y.Y. Liu, J. Chen, Y.Q. Wang, W.H. Zhu, T.F. Xie, Q.Q. Qiu, and T.X. Liang, Stable MOF-In_2S_3/ZnFe layered dioxide heterostructures for improving photocatalytic degradation: Degradation pathways, kinetics, and charge migration. Colloids. Surf. A.689 (2024) 133758. https://doi.org/10.1016/j.colsurfa.2024.133758

[6]. D.D. Yang, P.D. Hong, Y. Hu, Y.L. Li, C.M. Wang, J.Y. He, B. Sun, S.G. Zhu, L. T. Kong, and J.H. Liu, Carbon framework-encapsulated copper oxide particles to activate peroxymonosulfate for the efficient degradation of tetracycline. Appl. Surf. Sci. 552 (2021) 149424. https://doi.org/10.1016/j.apsusc.2021.149424

[7]. D. Li, H. Li, M. Long, X. Bai, Q. Zhao, Q. Wen, and F. Song, Synergetic effect of photocatalysis and peroxymonosulfate activation by MIL-53Fe@TiO_2 on efficient degradation of tetracycline hydrochloride under visible light irradiation. CrystEngComm. 24 (2022) 4283-4293. https://doi.org/10.1039/d2ce00372d

[8]. X. Peng, J. Wu, Z. Zhao, X. Wang, H. Dai, Y. Li, Y. Wei, G. Xu, and F. Hu, High efficiency degradation of tetracycline by peroxymonosulfate activated with Fe/NC

catalysts: Performance, intermediates, stability and mechanism. Environ. Res. 205 (2022) 112538. https://doi.org/10.1016/j.envres.2021.112538

[9]. P. Xu, S. Xie, X. Liu, L. Wang, R. Wu, and B. Hou, Efficient removal of tetracycline using magnetic $MnFe_2O_4/MoS_2$ nanocomposite activated peroxymonosulfate: Mechanistic insights and performance evaluation. Chem. Eng. J. 480 (2024) 148233. https://doi.org/10.1016/j.cej.2023.148233